

# Narrow-width approximation accuracy

C. F. Uhlemann<sup>1,\*</sup> and N. Kauer<sup>2,†</sup>

<sup>1</sup>*Institut für Theoretische Physik, Universität Würzburg, D-97074 Würzburg, Germany*

<sup>2</sup>*Department of Physics, Royal Holloway,  
University of London, Egham TW20 0EX, UK*

(Dated: January 27, 2009)

## Abstract

A study of general properties of the narrow-width approximation (NWA) with polarization/spin decorrelation is presented. We prove for sufficiently inclusive differential rates of arbitrary resonant decay or scattering processes with an on-shell intermediate state decaying via a cubic or quartic vertex that decorrelation effects vanish and the NWA is of order  $\Gamma$ . Its accuracy is then determined numerically for all resonant 3-body decays involving scalars, spin- $\frac{1}{2}$  fermions or vector bosons. We specialize the general results to MSSM benchmark scenarios. Significant off-shell corrections can occur – similar in size to QCD corrections. We qualify the configurations in which a combined consideration is advisable. For this purpose, we also investigate process-independent methods to improve the NWA.

PACS numbers: 25.75.Dw, 11.80.Fv, 12.60.-i

Keywords: resonant particle production; perturbative calculations; narrow-width approximation

---

\*uhlemann@physik.uni-wuerzburg.de

†n.kauer@rhul.ac.uk

## I. INTRODUCTION

Theoretical arguments and experimental observations indicate that new particles or interactions play an important role at the TeV scale, which will soon become directly accessible at the Large Hadron Collider (LHC). In the near future we can therefore anticipate groundbreaking discoveries that reveal physics beyond the Standard Model (BSM) [1]. Theoretically appealing extensions of the Standard Model often feature numerous additional interacting heavy particles. BSM phenomenology is hence characterized by particle production and cascade decays, which lead to many-particle final states and scattering amplitudes with complex resonance structure. In order to extract the additional Lagrangian parameters of an extended theory from collider data, theoretical predictions are required that match the experimental accuracies.

The treatment of unstable particles in quantum field theory is complicated by the absence of asymptotic final states for particles with finite mean lifetime. That a consistent theory respecting unitarity, renormalizability and causality can be formulated based on external stable states only has been shown in Ref. [2]. That work, however, does not discuss how to carry out fixed-order perturbative calculations involving unstable particles. Subsequently, several finite-width schemes have been discussed in the literature that in principle facilitate cross section calculations for arbitrary processes at tree [3] and loop level [4], where the full fixed-order scattering amplitude is taken into account.<sup>1</sup> If the width  $\Gamma$  of an unstable particle is much smaller than its mass  $M$ , amplitude contributions that feature the corresponding resonant intermediate state are generically enhanced by a factor of order  $M/\Gamma$ . A theoretically consistent method to extract this typically dominant part of the amplitude is provided by the narrow-width approximation (NWA) [6]. The NWA allows to neglect nonresonant as well as nonfactorizable amplitude contributions, thus leading to significant simplifications for calculations in extensions of the Standard Model or calculations of higher order corrections. When the NWA is applied in such calculations the unstable particle is effectively restricted to on-shell states. We note that the NWA is hence implicitly applied whenever branching ratios are extracted from reaction rates. Recently, it has been observed that the NWA can be unreliable in relevant circumstances, namely with decays where a

---

<sup>1</sup> A method for the inclusion of finite-width effects in event generators is discussed in Ref. [5].

daughter mass approaches the parent mass or when parton distribution functions are convolved with a resonant hard scattering process [7]. A more detailed study of the accuracy of the NWA is thus well motivated.

In Sec. II, we describe the NWA and clarify the treatment of polarization and spin correlations. We then consider correlation effects for decay and scattering rates in the special case of an on-shell intermediate state, which allows us to prove that the NWA error is of order  $\Gamma$ . To the best of our knowledge no proof for this result has previously been given in the literature. The polarization/spin decorrelation has been considered in Ref. [8]. The authors find a result similar to that derived in Sec. II B, but obtain it by performing the little-group integral for the resonant particle and assuming that the subamplitudes transform under some suitable representation of the little group. In our more direct derivation we will explicitly argue for the transformation of the subamplitudes and see that the full little-group integral is not generally required.

When applied in perturbative calculations, the uncertainty of the NWA is commonly estimated as between  $\approx \Gamma/M/3$  and  $\approx 3\Gamma/M$ , i.e. of order  $\Gamma/M$  in the physics sense. In Sec. III we test this assumption systematically for all resonant 3-body decays involving scalars, spin- $\frac{1}{2}$  fermions or vector bosons. We then specialize the generic results to benchmark scenarios in the Minimal Supersymmetric Standard Model (MSSM). Our findings in Sec. III naturally raise the question of process-independent improvements of the NWA, which we investigate in Sec. IV. We close with a summary in Sec. V.

## II. NWA PROPERTIES

### A. NWA definition

Formally, the NWA factorization into production of the unstable particle and its subsequent decay is obtained from the full cross section formula by factorizing the phase space and integrating out the Breit-Wigner resulting from the squared denominator of the resonant particle's propagator. With  $P$  denoting the sum of the incoming particles' momenta and  $q$  and  $p_i$  denoting the momenta of the intermediate resonant particle and the final state

particles, respectively, the phase-space factorization of the  $n$ -particle phase-space element

$$d\Phi_n(P; p_1, \dots, p_n) = (2\pi)^4 \delta^{(4)}(P - \sum_{i=1}^n p_i) \prod_{j=1}^n \frac{d^3 \vec{p}_j}{(2\pi)^3 2E_j}$$

into a  $j$ -particle phase-space element for the production process, an  $(n - j + 1)$ -particle phase-space element for the decay and an additional  $q^2$ -integration is given by

$$d\Phi_n(P; p_1, \dots, p_n) = d\Phi_j(P; p_1, \dots, p_{j-1}, q) \times \frac{dq^2}{2\pi} \times d\Phi_{n-j+1}(q; p_j, \dots, p_n). \quad (1)$$

Denoting the resonant particle's mass and width by  $M$  and  $\Gamma$ , respectively, the squared propagator denominator is given by  $D(q^2) := 1/[(q^2 - M^2)^2 + M^2\Gamma^2]$ . It is integrated out via

$$\begin{aligned} \int_{q_{\min}^2}^{q_{\max}^2} \frac{dq^2}{2\pi} D(q^2) \sigma_r(q^2) &\rightarrow \int_{-\infty}^{\infty} \frac{dq^2}{2\pi} D(q^2) \sigma_r(q^2) \\ &\rightarrow \frac{1}{2M\Gamma} \int dq^2 \delta(q^2 - M^2) \sigma_r(q^2) = \frac{\sigma_r(M^2)}{2M\Gamma}, \end{aligned} \quad (2)$$

where  $q_{\min, \max}^2$  are the kinematic bounds for  $q^2$  and  $\sigma_r(q^2)$  denotes the residual differential cross section (dependencies on quantities other than  $q^2$  have been suppressed). We note that the second and third expression are asymptotically equal for  $\Gamma \rightarrow 0$ . For finite  $\Gamma$ , Transformation (2) constitutes the core NWA. In the first step one assumes that adding the contributions from  $q^2$  regions that are not kinematically accessible has a negligible impact, which is the case if  $M^2$  is not close to  $q_{\min, \max}^2$  as measured by  $\Gamma$ . In the second step we assume that the  $q^2$ -dependence of the remaining integrand  $\sigma_r(q^2)$ , i.e. the residual squared amplitude and phase-space factors, is weak compared to that of the strongly peaked Breit-Wigner.

While the core NWA already provides considerable simplification, it does not facilitate complete factorization for nonscalar particles, since the production and decay process are linked by correlation effects. By additionally neglecting polarization/spin correlations between the production and decay parts we obtain the standard NWA. More specifically, the corresponding numerator of the squared matrix element is replaced for unstable vector bosons and fermions, i.e.

$$\begin{aligned} |\mathcal{M}_p^\mu(-g_{\mu\nu} + \frac{q_\mu q_\nu}{M^2}) \mathcal{M}_d^\nu|^2 &= |\sum_\lambda \mathcal{M}_p^\mu \epsilon_\mu^{*\lambda} \epsilon_\nu^\lambda \mathcal{M}_d^\nu|^2 \rightarrow \frac{1}{3} \sum_{\lambda_1, \lambda_2} |\mathcal{M}_p^\mu \epsilon_\mu^{*\lambda_1}|^2 |\epsilon_\nu^{\lambda_2} \mathcal{M}_d^\nu|^2, \\ |\mathcal{M}_p(\not{q} + M) \mathcal{M}_d|^2 &= |\sum_s \mathcal{M}_p u_s \bar{u}_s \mathcal{M}_d|^2 \rightarrow \frac{1}{2} \sum_{s_1, s_2} |\mathcal{M}_p u_{s_1}|^2 |\bar{u}_{s_2} \mathcal{M}_d|^2 \end{aligned} \quad (3)$$

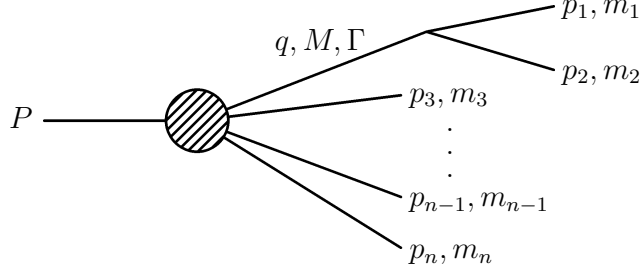


FIG. 1: Resonant decay or scattering process kinematics with total incoming momentum  $P$ .

with vector boson propagator in unitary gauge and suppressing the argument  $q$  for the polarization vectors and spinors. The resulting factorization of the cross section into  $\sigma_p \times \text{BR}$  constitutes the standard NWA factorization. Two sources of potential problems thus arise: the factorization of the squared amplitude neglects correlation effects, and off-shell effects are ignored when replacing the  $q^2$ -integration with a constant factor. We address the former issue in the next section.

## B. Polarization/spin decorrelation

In this section we show that there are no polarization/spin correlation effects for total or sufficiently inclusive differential rates<sup>2</sup> of arbitrary resonant decay or scattering processes with an on-shell intermediate state decaying via a cubic or quartic vertex. We consider processes with an unstable vector boson and note that a similar argument applies for unstable fermions. The squared amplitude for a process with resonant massive vector boson, which we assume to be on mass-shell, is given by

$$|\mathcal{M}_r|^2 = |\mathcal{M}_p^\mu(-g_{\mu\nu} + \frac{q_\mu q_\nu}{M^2})\mathcal{M}_d^\nu|^2,$$

where the denominator of the squared propagator is suppressed. By decoupling the polarization sum and inserting a polarization average, i.e. applying Transformation (3), one obtains the decorrelated squared matrix element

$$\overline{|\mathcal{M}_r|^2} = \left[ \mathcal{M}_p^\mu(-g_{\mu\nu} + \frac{q_\mu q_\nu}{M^2})\mathcal{M}_p^{\nu*} \right] \times \frac{1}{3} \left[ \mathcal{M}_d^\alpha(-g_{\alpha\beta} + \frac{q_\alpha q_\beta}{M^2})\mathcal{M}_d^{\beta*} \right].$$

<sup>2</sup> For a cubic (quartic) decay vertex,  $\theta_1$  ( $\theta_0$ ,  $\phi_0$  and  $\phi_1$ ) has to be integrated out. The angular variables are defined below Eq. (5).

As first step, we consider the process of Fig. 1, where the resonant particle is produced in an arbitrary process with total incoming momentum  $P$  and decays via a 2-body decay. To obtain the total rate for a specific process, the matrix elements have to be integrated over the full phase space. Here, we consider the total rate after application of Transformation (2), which – up to overall factors – is given by

$$\begin{aligned}
& \int \prod_{i=1}^n \frac{d^3 \vec{p}_i}{2E_i} \delta^{(4)}(P - \sum_{j=1}^n p_j) D(q^2) |\mathcal{M}_r|^2 \\
& \rightarrow \int \delta^{(4)}(P - q - \sum_{j=3}^n p_j) \frac{d^3 \vec{q}}{2E_q} \prod_{i=3}^n \frac{d^3 \vec{p}_i}{2E_i} \frac{\delta(q^2 - M^2) dq^2}{2M\Gamma} \delta^{(4)}(q - p_1 - p_2) \frac{d^3 \vec{p}_1}{2E_1} \frac{d^3 \vec{p}_2}{2E_2} |\mathcal{M}_r|^2 \\
& = \int \frac{\delta^{(4)}(P - q - \sum_{j=3}^n p_j)}{2M\Gamma} \frac{d^3 \vec{q}}{2E_q} \prod_{i=3}^n \frac{d^3 \vec{p}_i}{2E_i} \delta^{(4)}(q - p_1 - p_2) \frac{d^3 \vec{p}_1}{2E_1} \frac{d^3 \vec{p}_2}{2E_2} |\mathcal{M}_r|^2 \Big|_{q^2=M^2}.
\end{aligned}$$

The standard NWA is now obtained by decorrelating the squared amplitude, i.e. by replacing  $|\mathcal{M}_r|^2$  with  $\overline{|\mathcal{M}_r|^2}$ . To determine the effect of this procedure we consider the difference

$$\int \frac{\delta^{(4)}(P - q - \sum_{j=3}^n p_j)}{2M\Gamma} \frac{d^3 \vec{q}}{2E_q} \prod_{i=3}^n \frac{d^3 \vec{p}_i}{2E_i} \underbrace{\delta^{(4)}(q - p_1 - p_2) \frac{d^3 \vec{p}_1}{2E_1} \frac{d^3 \vec{p}_2}{2E_2} (|\mathcal{M}_r|^2 - \overline{|\mathcal{M}_r|^2})}_{=:H} \Big|_{q^2=M^2}. \quad (4)$$

Exploiting that  $H$  defined in Expression (4) is Lorentz invariant, we choose the Gottfried-Jackson frame [9], in which  $q = (E_q, \vec{0})^T$ , to evaluate it. In this frame our assumption  $q^2 = M^2$  implies  $q = (M, \vec{0})^T$ . By integrating out  $\vec{p}_2$  and substituting  $d^3 \vec{p}_1 = |\vec{p}_1|^2 d|\vec{p}_1| d\Omega_1$  we find

$$H = \int \frac{|\vec{p}_1|^2 d|\vec{p}_1|}{2E_1} \delta(E_q - E_1 - E_2) \underbrace{\int d\Omega_1 (|\mathcal{M}_r|^2 - \overline{|\mathcal{M}_r|^2})}_{=:I} \Big|_{\{\vec{p}_2 = -\vec{p}_1, E_q = M\}}. \quad (5)$$

We choose  $d\Omega_1$  as innermost integration, for which  $|\vec{p}_1|$  and  $\vec{p}_3, \dots, \vec{p}_n$  are invariables. Since the production and decay amplitudes  $\mathcal{M}_p^\mu \epsilon_\mu^*$  and  $\mathcal{M}_d^\nu \epsilon_\nu$  are Lorentz invariant,  $\mathcal{M}_p^\mu$  and  $\mathcal{M}_d^\nu$  are Lorentz 4-vectors. The spatial component of the decay (production) 4-vector has to be proportional to  $\vec{p}_1$  (a function of  $\vec{p}_3, \dots, \vec{p}_n$ ) since no independent other 4-vectors exist in the decay (production) part, i.e. with  $\mathcal{M}_p = (\mathcal{M}_p^0, \vec{\mathcal{M}}_p)^T$  and  $\mathcal{M}_d = (\mathcal{M}_d^0, \vec{\mathcal{M}}_d)^T$  we have  $\vec{\mathcal{M}}_d \propto \vec{p}_1$  and  $\vec{\mathcal{M}}_p$  fixed.<sup>3</sup> We therefore choose  $d\Omega_1 = d\cos\theta_1 d\phi_1$  with  $\theta_1 = \angle(\vec{p}_1, \vec{\mathcal{M}}_p)$ . Furthermore, in the Gottfried-Jackson frame the polarization sum  $-g_{\mu\nu} + q_\mu q_\nu / M^2$  is given

<sup>3</sup> The proportionality factor for  $\vec{\mathcal{M}}_d$  can depend on  $\vec{p}_i$  only through  $|\vec{p}_1|$ , which is fixed.

by  $\text{diag}(0, \mathbb{1}_3)$  and for the squared matrix elements we then get

$$|\mathcal{M}_r|^2 = |\vec{\mathcal{M}}_p \cdot \vec{\mathcal{M}}_d|^2 = |\vec{\mathcal{M}}_p|^2 |\vec{\mathcal{M}}_d|^2 \cos^2 \theta_1 \quad \text{and} \quad \overline{|\mathcal{M}_r|^2} = \frac{1}{3} |\vec{\mathcal{M}}_p|^2 |\vec{\mathcal{M}}_d|^2.$$

Evaluating  $I$  defined in Expression (5), we thus obtain

$$I = |\vec{\mathcal{M}}_p|^2 |\vec{\mathcal{M}}_d|^2 \int d\phi_1 \int_{-1}^1 d\cos\theta_1 \left( \cos^2 \theta_1 - \frac{1}{3} \right) = 0,$$

which proves that polarization decorrelation does not introduce an error for on-shell intermediate states in resonant processes of the type shown in Fig. 1.

We now consider the case where the unstable particle decays via a quartic vertex. More specifically, we consider the process of Fig. 1 with an additional particle with outgoing momentum  $p_0$  attached to the decay vertex connecting  $q$ ,  $p_1$  and  $p_2$ . Again, we consider a total or sufficiently inclusive differential rate after application of Transformation (2) and, similar to Eq. (5), arrive at

$$\begin{aligned} H &= \int \frac{d^3 \vec{p}_0}{2E_0} \frac{d^3 \vec{p}_1}{2E_1} \delta(E_q - \sum_{i=0}^2 E_i) \left( |\mathcal{M}_r|^2 - \overline{|\mathcal{M}_r|^2} \right) \Big|_{\{\vec{p}_2 = -\vec{p}_0 - \vec{p}_1, E_q = M\}} \\ &= \int \frac{|\vec{p}_0|^2 d|\vec{p}_0|}{2E_0} \frac{|\vec{p}_1|^2 d|\vec{p}_1|}{2E_1} d\cos\theta_1 \delta(E_q - \sum_{i=0}^2 E_i) \underbrace{\int d\cos\theta_0 d\phi_0 d\phi_1 \left( |\mathcal{M}_r|^2 - \overline{|\mathcal{M}_r|^2} \right)}_{=:J} \Big|_{\{\dots\}} \end{aligned}$$

as test for correlation effects. Now,  $|\vec{p}_0|$ ,  $|\vec{p}_1|$ ,  $\theta_1$  and  $\vec{\mathcal{M}}_p$  which, as before, is a function of  $p_3, \dots, p_n$  are fixed for the inner integrations over  $\theta_0$ ,  $\phi_0$  and  $\phi_1$ . We parameterized the  $\vec{p}_0$ -integration as  $d^3 \vec{p}_0 = |\vec{p}_0|^2 d|\vec{p}_0| d\cos\theta_0 d\phi_0$ , where the orientation of  $\vec{p}_0$  is measured relative to that of  $\vec{\mathcal{M}}_p$ , i.e.  $\theta_0 = \angle(\vec{p}_0, \vec{\mathcal{M}}_p)$ . The  $\vec{p}_1$ -integration was parameterized as  $d^3 \vec{p}_1 = |\vec{p}_1|^2 d|\vec{p}_1| d\cos\theta_1 d\phi_1$ , oriented such that  $\theta_1 = \angle(\vec{p}_1, \vec{p}_0)$ .  $\hat{r}_1$ , the unit vector in the direction of  $\vec{p}_1$ , is obtained from  $\hat{r}_0$ , the unit vector in the direction of  $\vec{p}_0$ , by first rotating by  $\theta_1$  around the axis defined by  $\hat{\phi}_0 = (-\sin\phi_0, \cos\phi_0, 0)^T$  and then by  $\phi_1$  around  $\hat{r}_0$ :

$$\vec{p}_1 = |\vec{p}_1| Q(\hat{r}_0, \phi_1) Q(\hat{\phi}_0, \theta_1) \hat{r}_0, \quad (6)$$

where  $Q(\vec{x}, \alpha)_{ij} = -\sum_k \epsilon_{ijk} x_k \sin\alpha + (\delta_{ij} - x_i x_j) \cos\alpha + x_i x_j$  is the matrix representing a rotation by the angle  $\alpha$  around the axis defined by the unit vector  $\vec{x} = (x_1, x_2, x_3)^T$ . Since the moduli of  $\vec{p}_0$  and  $\vec{p}_1$  as well as their relative orientation are fixed for the integrations in  $J$ , the decay matrix element can be decomposed as

$$\vec{\mathcal{M}}_d = c_0 \vec{p}_0 + c_1 \vec{p}_1 + c_2 \vec{p}_0 \times \vec{p}_1, \quad (7)$$

where we have exploited that the integration is performed in the Gottfried-Jackson frame and  $\vec{\mathcal{M}}_d$  can thus not depend on  $p_3, \dots, p_n$ . Note also that  $\vec{p}_2 = -\vec{p}_0 - \vec{p}_1$  is not an independent 3-vector and hence does not appear in the decomposition. The coefficients  $c_0$ ,  $c_1$  and  $c_2$  can only depend on  $|\vec{p}_0|$ ,  $|\vec{p}_1|$  or  $\vec{p}_0 \cdot \vec{p}_1$  (or equivalently  $\theta_1$ ). They are, however, independent of the variables of the  $J$ -integration  $\theta_0$ ,  $\phi_0$  and  $\phi_1$ . Using the explicit expressions of Eqs. (6) and (7),  $J$  can be evaluated, and we find  $J = 0$ . We conclude that also no error is introduced by decorrelation when the intermediate particle decays via a quartic vertex.

We now generalize the proof to an on-shell intermediate state decaying via a cubic or quartic vertex in an arbitrary resonant process, where the decay products of the unstable particle may decay further. Suppose the particle with momentum  $p_1$  decays into  $m$  particles with momenta  $p_{11}, \dots, p_{1m}$ . We map the kinematics of the extended process to the kinematic configuration of Fig. 1 and factorize the entire phase-space element by applying Eq. (1) to the intermediate state  $p_1$

$$d\Phi(P; \dots) = d\Phi(P; p_1, p_2, \dots, p_n) \frac{dp_1^2}{2\pi} d\Phi(p_1; p_{11}, \dots, p_{1m}).$$

By first integrating  $d\Phi(P; p_1, p_2, \dots, p_n)$ , we construct the situation that we dealt with before, the only difference being that in the decomposition of the matrix element  $\mathcal{M}_d$  we now have additional terms involving  $\vec{p}_{1i}$ ,  $i = 1, \dots, m$ . However, in the crucial inner integrations of  $d\Phi(P; p_1, p_2, \dots, p_n)$  the relative orientations of these momenta are fixed and thus they transform like  $\vec{p}_1$  under rotations. The absence of on-shell correlation effects can therefore be shown in the same way as above. Generalization to the case where multiple decay products decay further or where correlation effects for multiple on-shell intermediate states are considered is straightforward. Note that this extension again holds not only for total rates, but also for sufficiently inclusive differential rates.

### C. Order of the NWA error

We can now prove that the relative error

$$R = \frac{\Gamma_{\text{OFS}} - \Gamma_{\text{NWA}}}{\Gamma_{\text{NWA}}} \quad (8)$$



is of  $\mathcal{O}(\Gamma)$  for the decay and scattering rates considered in Sec. II B.<sup>4</sup> A priori this is not clear. The error as function of  $\Gamma$  could, for example, behave like  $\Gamma^\kappa$  with  $0 < \kappa < 1$ . In this case, a series expansion around  $\Gamma = 0$  would be invalid. We consider the off-shell decay rate

$$\Gamma_{\text{OFS}} = \int_{q_{\text{min}}^2}^{q_{\text{max}}^2} \frac{dq^2}{2\pi} D(q^2, \Gamma) \Gamma_r(q^2),$$

where kinematic limits define the integration bounds  $q_{\text{min,max}}^2$  and we have explicitly noted the dependence of the squared propagator denominator on  $\Gamma$ .  $\Gamma_r(q^2)$  denotes the residual,  $\Gamma$ -independent integrand.<sup>5</sup> More specifically,  $\Gamma_r$  is the squared combination of the production matrix element, the numerator of the propagator and the decay matrix element, integrated over  $d\Phi_p$  and  $d\Phi_d$  and includes overall factors like  $1/(2\sqrt{P^2})$ . The decay rate in NWA is given by  $\Gamma_{\text{NWA}} = \Gamma_p(M^2) \times \Gamma_d(M^2)/\Gamma$  where  $\Gamma_p$  and  $\Gamma_d$  are the production rate and partial decay rate, respectively. We can now write:

$$\begin{aligned} \Gamma_{\text{OFS}} - \Gamma_{\text{NWA}} &= \int_{q_{\text{min}}^2}^{q_{\text{max}}^2} \frac{dq^2}{2\pi} D(q^2, \Gamma) \Gamma_r(q^2) - \frac{\Gamma_p(M^2) \Gamma_d(M^2)}{\Gamma} \\ &= \int_{q_{\text{min}}^2}^{q_{\text{max}}^2} \frac{dq^2}{2\pi} D(q^2, \Gamma) (\Gamma_r(q^2) - \Gamma_p(M^2) 2M \Gamma_d(M^2)) - \alpha(\Gamma) \frac{\Gamma_p(M^2) \Gamma_d(M^2)}{\Gamma} \\ &\stackrel{(*)}{=} \int_{q_{\text{min}}^2}^{q_{\text{max}}^2} \frac{dq^2}{2\pi} D(q^2, \Gamma) (\Gamma_r(q^2) - \Gamma_r(M^2)) - \alpha(\Gamma) \frac{\Gamma_p(M^2) \Gamma_d(M^2)}{\Gamma} \end{aligned}$$

with  $\alpha := 1 - 2M\Gamma \int_{q_{\text{min}}^2}^{q_{\text{max}}^2} D(q^2, \Gamma) dq^2 / (2\pi)$ . Note that  $\alpha = 0$  for  $q_{\text{min,max}}^2 = \pm\infty$ . As shown in Sec. II B, decorrelation effects vanish and  $\Gamma_r(M^2)$  factorizes, which has been used in (\*).

For the relative deviation  $R$  we get

$$|R| = \left| \frac{\Gamma_{\text{OFS}} - \Gamma_{\text{NWA}}}{\Gamma_{\text{NWA}}} \right| \leq \left| \int_{q_{\text{min}}^2}^{q_{\text{max}}^2} \frac{dq^2}{2\pi} D(q^2, \Gamma) \Gamma \frac{\Gamma_r(q^2) - \Gamma_r(M^2)}{\Gamma_p(M^2) \Gamma_d(M^2)} \right| + |\alpha(\Gamma)|.$$

Assume now that  $\Gamma_r(q^2)$  is twice continuously differentiable in the kinematically allowed phase-space region and that  $\Gamma_p(q^2) \Gamma_d(q^2) = 0 \Leftrightarrow q^2 \in \{q_{\text{min}}^2, q_{\text{max}}^2\}$ . Then, the function

$$g_M(q^2) := \frac{\Gamma_r(q^2)}{\Gamma_p(M^2) \Gamma_d(M^2)} \tag{9}$$

<sup>4</sup> We illustrate the proof using total decay rates, but note that it also applies to sufficiently inclusive differential decay and scattering rates as considered in Sec. II B.

<sup>5</sup> Since interference effects with nonresonant diagrams are not resonance enhanced, we do not consider them here.

is twice continuously differentiable with respect to  $q^2$  for all  $q^2 \in [q_{\min}^2, q_{\max}^2]$  and  $M^2 \in (q_{\min}^2, q_{\max}^2)$ , which we assume in the following, since we consider resonant intermediate states. By second order Taylor expansion we then get

$$g_M(q^2) = g_M(M^2) + g'_M(M^2) \cdot (q^2 - M^2) + \frac{1}{2}g''_M(x) \cdot (q^2 - M^2)^2$$

with  $x \in [q_{\min}^2, q_{\max}^2]$ . Note that  $x$  depends on  $q^2$ . As continuous functions on the compact set  $[q_{\min}^2, q_{\max}^2]$ ,  $g'_M$  and  $g''_M$  are then bounded and we can find  $L_1 > 0$  and  $L_2 > 0$  such that

$$|g'_M(q^2)| \leq L_1 \quad \text{and} \quad |g''_M(q^2)| \leq L_2 \quad \forall q^2 \in [q_{\min}^2, q_{\max}^2]. \quad (10)$$

We can now further evaluate  $|R|$  to obtain

$$\begin{aligned} |R| &\leq \left| \int_{q_{\min}^2}^{q_{\max}^2} \frac{dq^2}{2\pi} D(q^2, \Gamma) \Gamma (g_M(q^2) - g_M(M^2)) \right| + |\alpha(\Gamma)| \\ &= \frac{\Gamma}{2\pi} \left| \int_{q_{\min}^2}^{q_{\max}^2} dq^2 D(q^2, \Gamma) \left( g'_M(M^2) \cdot (q^2 - M^2) + \frac{1}{2}g''_M(x) \cdot (q^2 - M^2)^2 \right) \right| + |\alpha(\Gamma)| \\ &\leq \frac{\Gamma L_1}{2\pi} \left| \int_{q_{\min}^2}^{q_{\max}^2} dq^2 \frac{q^2 - M^2}{(q^2 - M^2)^2 + M^2\Gamma^2} \right| + \frac{\Gamma L_2}{4\pi} \int_{q_{\min}^2}^{q_{\max}^2} dq^2 \left| \frac{(q^2 - M^2)^2}{(q^2 - M^2)^2 + M^2\Gamma^2} \right| + |\alpha(\Gamma)| \\ &= \frac{\Gamma L_1}{4\pi} \left| \log \frac{(q_{\max}^2 - M^2)^2 + M^2\Gamma^2}{(q_{\min}^2 - M^2)^2 + M^2\Gamma^2} \right| \\ &\quad + \frac{\Gamma L_2}{4\pi} \left| q_{\max}^2 + M\Gamma \arctan \frac{M^2 - q_{\max}^2}{M\Gamma} - q_{\min}^2 - M\Gamma \arctan \frac{M^2 - q_{\min}^2}{M\Gamma} \right| + |\alpha(\Gamma)|. \end{aligned}$$

By employing the Taylor expansions

$$\begin{aligned} \log \frac{k + x^2}{l + x^2} &= \log \frac{k}{l} + \mathcal{O}(x^2), \\ \arctan \frac{k}{x} &= \text{sign}(k) \frac{\pi}{2} - \frac{x}{k} + \mathcal{O}(x^3) \end{aligned}$$

for small positive  $x$  to expand the log and arctan functions for small  $\Gamma$ , we get

$$|R| \leq \frac{\Gamma L_1}{4\pi} \left| \log \frac{(q_{\max}^2 - M^2)^2}{(M^2 - q_{\min}^2)^2} \right| + |\alpha(\Gamma)| + \frac{\Gamma L_2}{4\pi} (q_{\max}^2 - q_{\min}^2 + \pi M\Gamma) + \mathcal{O}(\Gamma^2).$$

Lastly, we evaluate and expand  $\alpha$ :

$$\begin{aligned} \alpha &= 1 - 2M\Gamma \int_{q_{\min}^2}^{q_{\max}^2} \frac{dq^2}{2\pi} D(q^2, \Gamma) = 1 - \frac{1}{\pi} \left( \arctan \frac{q_{\max}^2 - M^2}{M\Gamma} - \arctan \frac{q_{\min}^2 - M^2}{M\Gamma} \right) \\ &= \frac{M\Gamma}{\pi} \frac{(q_{\max}^2 - q_{\min}^2)}{(q_{\max}^2 - M^2)(M^2 - q_{\min}^2)} + \mathcal{O}(\Gamma^3), \end{aligned}$$

and obtain as final result:

$$\begin{aligned} \frac{|R|}{\Gamma} &\leq \frac{L_1}{4\pi} \left| \log \frac{(q_{\max}^2 - M^2)^2}{(q_{\min}^2 - M^2)^2} \right| + \frac{L_2}{4\pi} (q_{\max}^2 - q_{\min}^2) \\ &+ \frac{M}{\pi} \frac{(q_{\max}^2 - q_{\min}^2)}{(q_{\max}^2 - M^2)(M^2 - q_{\min}^2)} + \mathcal{O}(\Gamma), \end{aligned} \quad (11)$$

where  $L_1$  and  $L_2$  are  $\Gamma$ -independent constants with mass dimension  $-1$  and  $-3$ , respectively. We have thus shown that  $R$  is of  $\mathcal{O}(\Gamma)$  if  $M$  is in the interior of the kinematically allowed region.  $R/\Gamma$  is then finite in the limit  $\Gamma \rightarrow 0$ . Note that this is a stronger statement than the asymptotic equality of  $\Gamma_{\text{OFS}}$  and  $\Gamma_{\text{NWA}}$  for  $\Gamma \rightarrow 0$ , which immediately follows from the asymptotic equality of the off-shell and core NWA expressions (see Transformation (2)) and the absence of on-shell correlation effects.  $R = \mathcal{O}(\Gamma)$  does, however, not guarantee that  $|R| \approx \Gamma/M$  as suggested by the scales that occur in the unstable particle propagator. The leading terms in  $\Gamma$  on the right-hand side of Ineq. (11), while  $\Gamma$ -independent, may nevertheless become arbitrarily large as  $M$  approaches the kinematic limits. This can be seen directly by inspecting the factors that are explicitly  $(q_{\min, \max}^2 - M^2)$  dependent, but is also due to the fact that  $L_1$  and  $L_2$  may become large as  $M^2$  approaches  $q_{\min}^2$  or  $q_{\max}^2$ .

### III. NWA ACCURACY FOR RESONANT THREE-BODY DECAYS

In Sec. II we have already determined several necessary conditions for a small relative NWA error  $|R|$ : The standard NWA will only be accurate if polarization/spin correlation effects can be neglected. Furthermore, Transformation (2) shows that  $|(q_{\min, \max}^2)^{1/2} - M| \gtrsim \Gamma$  is necessary to effectively eliminate the dependence on the  $q^2$ -integration bounds. In the next section we systematically explore NWA deviations for the process class that allows application of the NWA while featuring minimal complexity in order to identify other accuracy limiting factors.

#### A. Model-independent analysis

We have systematically probed the NWA accuracy for resonant 3-body decays involving scalars, spin- $\frac{1}{2}$  fermions or vector bosons. By inserting these particles into the topology of Fig. 2 one obtains 48 generic decay processes. A particular process is selected by giving type

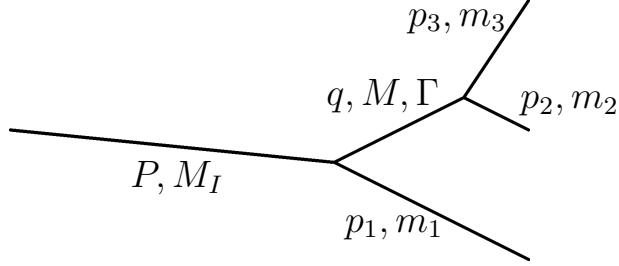


FIG. 2: Resonant 3-body decay kinematics.

(4-momentum, mass) for each particle:

$$T_I(P_I, M_I) \rightarrow T_1(p_1, m_1), T(q, M) \quad \text{and} \quad T(q, M) \rightarrow T_2(p_2, m_2), T_3(p_3, m_3),$$

where type can be scalar (S), fermion (F) or vector boson (V). The width of the intermediate particle with momentum  $q$  is  $\Gamma$ . We have created a custom, model-independent program that allows to calculate total decay rates with and without NWA for all 48 processes. The program has been validated using `SMadGraph` [10] and `SDECAY` [11].<sup>6</sup> Using this program, we scanned the parameter space for large values of  $|R|$  by varying masses, width and couplings. Note that coupling constants typically cancel in  $R$  with the exception of the relative strength of the chiral components of SFF and VFF vertices. This dependence has been taken into account in the scan. Qualitatively, we find that the NWA error will exceed order  $\Gamma/M$  for mass configurations in an extended vicinity of kinematic bounds, but not for sufficiently central configurations. A detailed description and discussion of the scan and its results can be found in Ref. [13]. Here, we choose the process that features the largest deviations, SSS-SSV, to explain the mechanism that can lead to large deviations even when the  $q^2$ -integral is not noticeably cut off by kinematic bounds. The largest deviations occur when all but one final state mass are small. We therefore set  $m_1 = m_2 = 0$ , but keep  $m_3 \neq 0$ . The  $q^2$ -integrand for this process is then given by

$$\left(1 - \frac{q^2}{M_I^2}\right) \left(1 - \frac{m_3^2}{q^2}\right) \left(\frac{(q^2 - m_3^2)^2}{m_3^2}\right) \frac{1}{(q^2 - M^2)^2 + M^2\Gamma^2}, \quad (12)$$

where the 1st- and 2nd-stage decay phase-space elements contribute the first and second factor, respectively, and the 2nd-stage decay matrix element gives the third factor. When

---

<sup>6</sup> Unitary gauge has been applied throughout. The employed Feynman rules have been double-checked using Ref. [12].

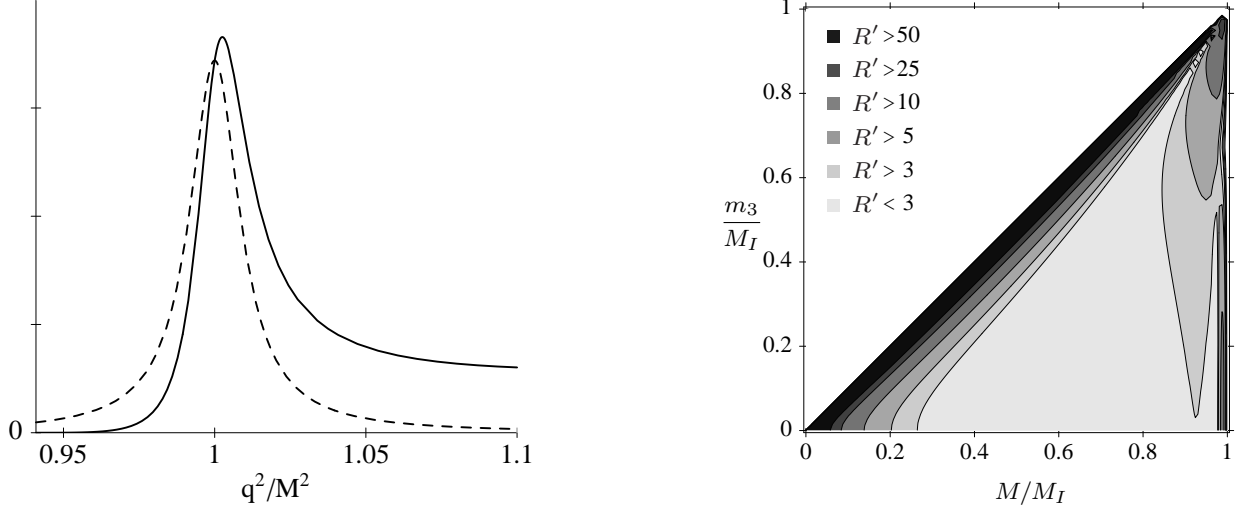


FIG. 3: Resonant  $1 \rightarrow 3$  decay SSS-SSV (see main text): The graph displays the  $q^2$ -dependence of the Breit-Wigner that is integrated out in the NWA (dashed) and of the complete integrand of Eq. (12) (solid) for  $m_3 = M - 3\Gamma$ . The contour plot shows  $R' := |R|/(\Gamma/M)$ , i.e. the magnitude of the relative NWA error in units of  $\Gamma/M$ , as function of  $m_3$  and  $M$  with  $m_1 = m_2 = 0$ . The width-mass ratio  $\Gamma/M$  is 0.01.

$m_3^2 \lesssim M^2$  the second and third factor effect a strong deformation of the Breit-Wigner shape, which, together with the resulting large NWA deviations, is displayed in Fig. 3. The deviation grows with increasing power of the deforming factors. When  $M$  approaches the lower kinematic bound,  $|R|$  is sensitive to the type of the 2nd-stage decay, which determines the power of the factor that deforms the Breit-Wigner peak. While this factor enhances the Breit-Wigner tail, the factor of the 1st-stage decay suppresses it. And vice versa for the upper bound. Generally, we find stronger effects for SSV, VSV, FFV, VVV and SVV than for FSF, SFF, VFF, VSS and SSS vertices. As mentioned above, coupling parameters do not affect the relative NWA error if they factorize. However, for processes with SFF or VFF vertices, a strong dependence on the relative strength of the chiral components can exist. In Fig. 4, we demonstrate this for the FFV-VFF decay. We conclude this section with a caveat:  $\Gamma_{\text{OFS}}$  has been calculated including the full range of invariant masses  $q^2$  for the intermediate resonant state. In a model-independent analysis we could, however, not take into account interference with amplitude contributions with different resonance structure or with nonresonant diagrams. In gauge theories, such contributions can in principle be important. In the next section we will consider examples in specific models.

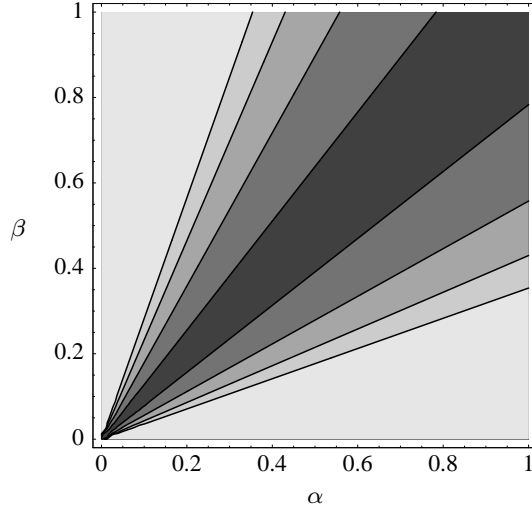


FIG. 4: Dependence of the magnitude of the relative NWA error  $R'$  (see Fig. 3) on the strength of the chiral components of the 1st-stage decay vertex  $\gamma^\mu(\alpha P_L + \beta P_R)$  for process FFV-VFF at the parameter point  $M/M_I = 0.68$ ,  $m_1/M_I = 0.3$  and  $m_2 = m_3 = 0$  with  $\Gamma/M = 0.01$ . Color code as in Fig. 3.

## B. MSSM analysis

We now specialize our model-independent analysis to benchmark scenarios in the MSSM. We determine for each  $1 \rightarrow 3$  decay<sup>7</sup> in the MSSM and each benchmark parameter point of the Snowmass Points and Slopes (SPS) [14] whether the resulting process is resonant, in which case the NWA accuracy  $R$  of Eq. (8) is calculated. The SPS mass spectra and decay widths have been generated using `SOFTSUSY` [15] and `SDECAY`, respectively. As example, we select the most thoroughly studied point SPS 1a (defined by the parameter set  $M_0 = 100$  GeV,  $M_{1/2} = 250$  GeV,  $A_0 = -100$  GeV,  $\tan\beta = 10$ ,  $\mu > 0$ ) and display in Table I resonant 3-body decay modes with  $|R| > 5\Gamma/M$  for which the distance between  $M$  and kinematic bounds is larger than 5 widths. Note that for  $\tilde{b}_1 \rightarrow W^- \tilde{t}_1 \rightarrow W^- b \tilde{\chi}_2^+$  the NWA error  $R$  is negative. All other processes in Table I have positive  $R$ . A complete listing of results with  $|R| > 5\Gamma/M$  can be found in Ref. [13].

The tabulated results are intended as guideline to alert the NWA user of potential large errors. In such cases a more detailed on-/off-shell comparison including all amplitude con-

<sup>7</sup> We consider final states with stable particles and up to one unstable particle. This is of interest, since subsequent decays do not generally mitigate the deviations [7].

TABLE I: Resonant 3-body decay modes in the MSSM at SPS 1a, for which  $R'$ , i.e. the magnitude of the relative NWA error in units of  $\Gamma/M$  (see Fig. 3) is larger than 5, and  $\Delta := \min(M_I - m_1 - M, M - m_2 - m_3)/\Gamma$ , i.e. the minimal distance between  $M$  and the kinematic bounds  $(q_{\min, \max}^2)^{1/2}$  in units of  $\Gamma$ , is larger than 2.

process	$R'$	$\Gamma/M$ [%]	$\Delta$
$H^+ \rightarrow \tilde{\tau}_1^* \tilde{\nu}_\tau \rightarrow \tilde{\tau}_1^* \tau \tilde{\chi}_1^+$	284	0.080	8.4
$\tilde{\chi}_1^+ \rightarrow \tilde{\chi}_1^0 W^+ \rightarrow \tilde{\chi}_1^0 e^+ \nu_e$	5.21	2.5	2.6
$\tilde{\chi}_1^+ \rightarrow \tilde{\chi}_1^0 W^+ \rightarrow \tilde{\chi}_1^0 u \bar{d}$	5.21	2.5	2.6
$\tilde{\chi}_2^+ \rightarrow e^+ \tilde{\nu}_e \rightarrow e^+ e^- \tilde{\chi}_1^+$	180	0.081	24
$\tilde{\chi}_3^0 \rightarrow \bar{\nu}_e \tilde{\nu}_e \rightarrow \bar{\nu}_e \nu_e \tilde{\chi}_2^0$	125	0.081	28
$\tilde{\chi}_3^0 \rightarrow \bar{\nu}_e \tilde{\nu}_e \rightarrow \bar{\nu}_e e^- \tilde{\chi}_1^+$	168	0.081	24
$\tilde{\chi}_4^0 \rightarrow \nu_e \tilde{\nu}_e \rightarrow \nu_e \nu_e \tilde{\chi}_2^0$	135	0.081	28
$\tilde{\chi}_4^0 \rightarrow \nu_e \tilde{\nu}_e \rightarrow \nu_e e \tilde{\chi}_1^+$	181	0.081	24
$\tilde{b}_1 \rightarrow W^- \tilde{t}_1 \rightarrow W^- b \tilde{\chi}_2^+$	10.1	0.51	7.7
$\tilde{g} \rightarrow d \tilde{d}_L^* \rightarrow d \tilde{\chi}_1^0$	9.54	0.94	7.4
$\tilde{g} \rightarrow d \tilde{d}_L^* \rightarrow d \tilde{\chi}_2^0$	7.89	0.94	7.4
$\tilde{t}_1 \rightarrow b \tilde{\chi}_2^+ \rightarrow b \tilde{e}_L^* \nu_e$	25.4	0.66	6.2
$\tilde{t}_1 \rightarrow b \tilde{\chi}_2^+ \rightarrow b \tilde{\nu}_e e^+$	28.1	0.66	6.2
$\tilde{t}_1 \rightarrow b \tilde{\chi}_2^+ \rightarrow b \tilde{\nu}_\tau \tau^+$	25.7	0.66	6.2

tributions is called for. We exemplify this by discussing two specific cases. The first process is  $\tilde{g} \rightarrow \tilde{\chi}_1^0 d \bar{d}$ , which proceeds via intermediate  $\tilde{d}_{L,R}$  states (see Fig. 5). At SPS 1a, one has  $M_{\tilde{g}} = 607.7$  GeV,  $M_{\tilde{d}_R} = 545.2$  GeV,  $M_{\tilde{d}_L} = 568.4$  GeV and  $M_{\tilde{\chi}_1^0} = 96.7$  GeV, which implies that all intermediate states can be on-shell. As seen in Table I, one finds  $R \approx 10 \Gamma/M$  for the graph with intermediate  $\tilde{d}_L$ .<sup>8</sup> In contrast, the graph with intermediate  $\tilde{d}_R$  is not affected by an unexpectedly large NWA error ( $R \approx 2 \Gamma/M$ ). This can be traced to the fact that  $\tilde{d}_L$

<sup>8</sup> Note the equality of the total decay rates with intermediate  $\tilde{d}_{L,R}$  and  $\tilde{d}_{L,R}^*$  state due to the  $C$  invariance of  $|\mathcal{M}|^2$ .

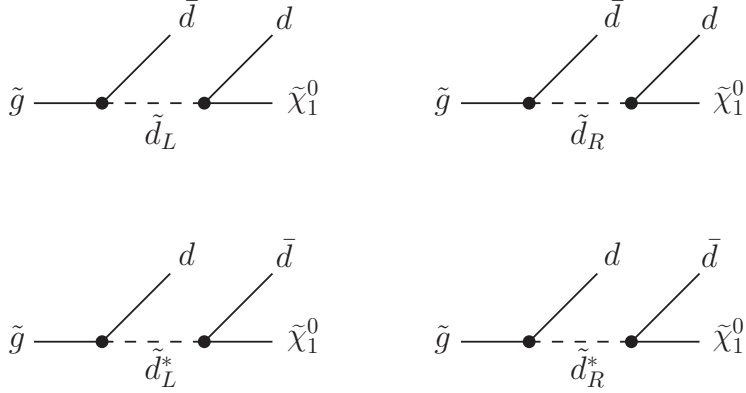


FIG. 5: Complete set of Feynman graphs for the MSSM 3-body decay  $\tilde{g} \rightarrow \tilde{\chi}_1^0 d \bar{d}$ .

has a much higher decay probability than  $\tilde{d}_R$  due to the chiral structure of the chargino and neutralino couplings. Consequently, the total width over mass ratio is about 1% for  $\tilde{d}_L$ , but only about 0.05% for  $\tilde{d}_R$ , i.e. in the latter case  $|(q_{\min, \max}^2)^{1/2} - M| > 200\Gamma$  and hence the absence of large NWA errors. When also taking into consideration the much larger resonant enhancement for the  $\tilde{d}_R$  in comparison with the  $\tilde{d}_L$  mediated process, one can expect that the former process in NWA provides a good approximation to the full  $\tilde{g} \rightarrow \tilde{\chi}_1^0 d \bar{d}$  rate. When calculated in NWA, the decay rate of the  $\tilde{d}_L$  mediated process is indeed approximately 100 times smaller than the decay rate of the  $\tilde{d}_R$  mediated process. Under these circumstances interference effects are likely to provide the leading correction to the NWA estimate. Interference between amplitudes with intermediate states related by charge conjugation is Breit-Wigner suppressed, because almost always either the invariant mass of  $\tilde{\chi}_1^0 d$  or  $\tilde{\chi}_1^0 \bar{d}$  will be close to  $M$ , i.e. only one of the propagators will be resonant. Furthermore, interference between amplitudes with  $\tilde{d}_L$  and  $\tilde{d}_R$  intermediate states is highly suppressed, since the overlap of the corresponding resonances is negligible:  $M_{\tilde{d}_L} - M_{\tilde{d}_R} \gg \Gamma_{\tilde{d}_L} + \Gamma_{\tilde{d}_R}$ . We computed the total decay rate for  $\tilde{g} \rightarrow \tilde{\chi}_1^0 d \bar{d}$  by Monte-Carlo integration of the `SMadGraph`-generated complete matrix element. Comparing this off-shell result to the NWA result for the  $\tilde{d}_R$  contribution, we find a relative deviation of 1.2%, which confirms our expectation.

As second example, we consider the process  $\tilde{\chi}_1^+ \rightarrow \tilde{\chi}_1^0 u \bar{d}$ , which proceeds via intermediate  $W^+$ ,  $\tilde{u}_L$  and  $\tilde{d}_L^*$  states (see Fig. 6). At SPS 1a, one has  $M_{\tilde{\chi}_1^+} = 181.7$  GeV,  $M_{\tilde{\chi}_1^0} = 96.7$  GeV,  $M_W = 79.8$  GeV,  $M_{\tilde{u}_L} = 561.1$  GeV and  $M_{\tilde{d}_L} = 568.4$  GeV, which implies that only



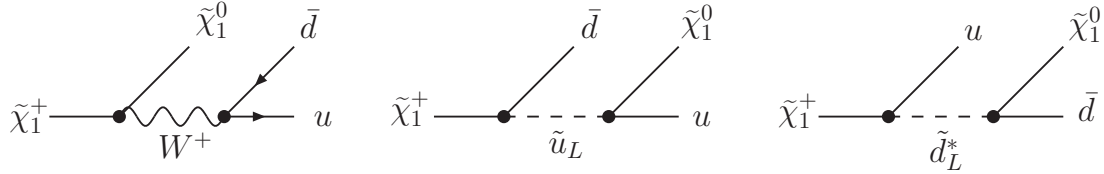


FIG. 6: Complete set of Feynman graphs for the MSSM 3-body decay  $\tilde{\chi}_1^+ \rightarrow \tilde{\chi}_1^0 u \bar{d}$ .

the intermediate  $W^+$  state can be on-shell. For the 1st-stage decay  $\tilde{\chi}_1^+ \rightarrow \tilde{\chi}_1^0 W^+$  with<sup>9</sup> BR = 7.5% the minimal distance to the kinematic bounds is  $M_I - m_1 - M = 2.6\Gamma$ , which is not large enough to rule out an unexpectedly large NWA error. In fact, Table I shows that  $R = 13\% = 5.2\Gamma/M$  for  $\tilde{\chi}_1^+ \rightarrow \tilde{\chi}_1^0 W^+ \rightarrow \tilde{\chi}_1^0 u \bar{d}$ . Primarily via interference the nonresonant  $\tilde{u}_L$  and  $\tilde{d}_L^*$  contributions slightly reduce the NWA error to  $R = 11\%$ , where the total decay rate for  $\tilde{\chi}_1^+ \rightarrow \tilde{\chi}_1^0 u \bar{d}$  with complete matrix elements is compared to the  $\tilde{\chi}_1^+ \rightarrow \tilde{\chi}_1^0 W^+ \rightarrow \tilde{\chi}_1^0 u \bar{d}$  rate in NWA. Since the 1st-decay stage is not affected by QCD corrections, this NWA error is particularly significant.

#### IV. PROCESS-INDEPENDENT NWA IMPROVEMENT

In this section we propose a modified NWA prescription that preserves the simplifying NWA features and improves the behavior close to kinematic bounds by taking into account phase-space properties. The standard NWA is obtained by replacing the distribution  $\psi : f \mapsto \int \frac{dq^2}{2\pi} D(q^2) f(q^2)$ , which – acting on the residual differential cross section  $\sigma_r$  – gives the total cross section<sup>10</sup>, by a rescaled Dirac distribution, i.e.

$$\psi(\sigma_r) = \int \frac{dq^2}{2\pi} D(q^2) \sigma_r(q^2) \quad \rightarrow \quad \psi_{\text{NWA}}(\sigma_r) = \frac{1}{2M\Gamma} \int dq^2 \delta(q^2 - M^2) \sigma_r(q^2), \quad (13)$$

which is motivated by the observation that the Breit-Wigner shape suppresses the contributions with  $q^2 \neq M^2$ . That is, for small  $\Gamma$ ,  $\psi$  essentially eliminates all contributions of  $f(q^2)$  except for the on-shell part, and in the limit  $\Gamma \rightarrow 0$ ,  $\psi(\sigma_r)$  and  $\psi_{\text{NWA}}(\sigma_r)$  are asymptotically equal.

However, for finite  $\Gamma$  the  $q^2$ -dependence of the phase-space factors and residual matrix elements can cause a significant deformation of the shape of  $D(q^2)\sigma_r(q^2)$  relative to the

<sup>9</sup> At SPS1a' [16] the branching ratio is 1.3%.

<sup>10</sup> Application to cross sections and decay rates is analogous.

Breit-Wigner shape  $D(q^2)$ , resulting in a considerable shift of the maximum position and maximal value. The effect is particularly strong when  $M$  is close to the kinematic bounds, where threshold-type factors suppress the resonant contribution and shift the maximum. Focusing on the impact of the  $q^2$ -dependence of the process-independent phase-space factors, we write  $\psi(\sigma_r) = \int \frac{dq^2}{2\pi} D(q^2) \text{PS}(q^2) \tilde{\sigma}_r(q^2)$ , where  $\text{PS}(q^2)$  denotes the integrand factor arising from the phase-space element. Even though the  $q^2$ -dependence of  $\text{PS}(q^2)$  deforms the Breit-Wigner, the shape of  $D(q^2)\text{PS}(q^2)$  is also strongly peaked and thus suggests a NWA-inspired approximation, which takes into account the shift of the maximum position caused by  $\text{PS}(q^2)$ . More specifically, we propose to substitute the mass of the resonance  $M$  with an effective mass  $M_{\text{eff}}$  in  $\psi_{\text{NWA}}(\sigma_r)$ . In analogy to  $M^2$  being the maximum position of the Breit-Wigner,  $M_{\text{eff}}^2$  is given by the position of the maximum of  $D(q^2)\text{PS}(q^2)$ :

$$\begin{aligned} \psi_{\text{NWA}}(\sigma_r) \quad \rightarrow \quad \psi_{\text{PSINWA}}(\sigma_r) &= \frac{1}{2M_{\text{eff}}\Gamma} \int dq^2 \delta(q^2 - M_{\text{eff}}^2) \sigma_r(q^2) \\ \text{with } M_{\text{eff}} &:= \left( \arg \max_{q^2} D(q^2)\text{PS}(q^2) \right)^{1/2}. \end{aligned} \quad (14)$$

The thus defined effective mass only exploits kinematic information and is hence universal for the class of processes with identical phase-space properties.<sup>11</sup> Due to  $\lim_{\Gamma \rightarrow 0} M_{\text{eff}} = M$ , the deviation of the effective mass from the physical mass is negligible unless  $M$  is close to the kinematic bounds. Therefore, the proposed phase-space improved narrow-width approximation (PSINWA) does not result in significant deviations in cases where the standard NWA gives  $\mathcal{O}(\Gamma/M)$ -accurate results. On the other hand, when  $M$  approaches a kinematic bound the behavior is improved: Since the distance between  $M_{\text{eff}}$  and the bound stays finite the PSINWA result does not vanish. The PSINWA error is therefore bounded in contrast to the diverging standard NWA error.

To exemplify this method, we consider the scalar resonant 3-body decay SSS-SSS (see Sec. III A). With  $\beta(m, M) := \sqrt{1 - m^2/M^2}$  and kinematic conventions as in Fig. 2, the 3-particle phase-space element is given by

$$d\phi = d\phi_p \frac{dq^2}{2\pi} d\phi_d,$$

<sup>11</sup> Since  $M_{\text{eff}}^2$  can be obtained by numerical, one-dimensional maximization of  $D(q^2)\text{PS}(q^2)$  with  $q^2 = M^2$  as suitable initial value, the computational complexity of its determination is negligible. In theories with mass relations it may be necessary to adjust other parameters to maintain theoretical properties like gauge invariance.

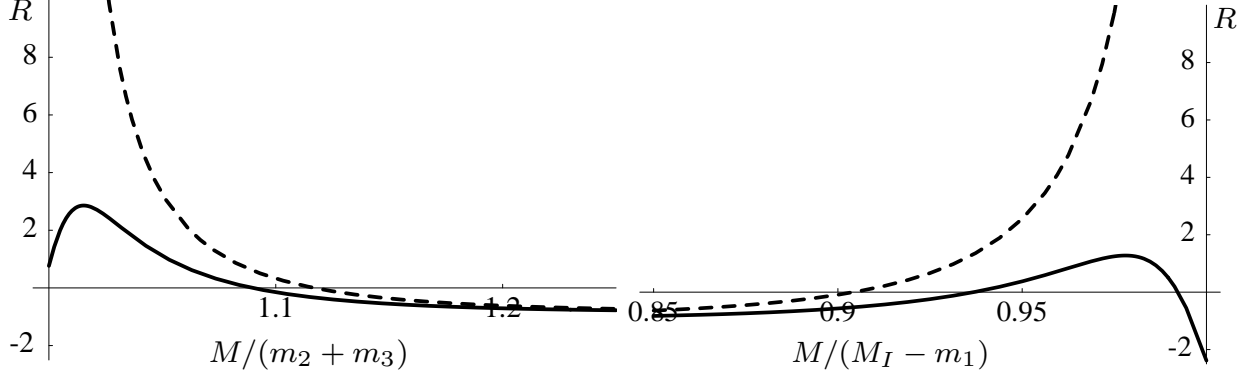


FIG. 7: Comparison of the phase-space improved (solid) and standard (dashed) NWA error for a scalar resonant 3-body decay, i.e. process SSS-SSS of Sec. III A, when the resonance mass  $M$  approaches the kinematic bounds  $m_2 + m_3$  (left) and  $M_I - m_1$  (right) (see Fig. 2). Displayed is the relative approximation error in units of resonance width/mass, i.e.  $R = (\Gamma_{\text{OFS}}/\Gamma_{[\text{PSI}] \text{NWA}} - 1)/(\Gamma/M)$ , for  $\Gamma/M = 0.05$ ,  $m_1 = m_2 = 0$  and  $m_3/M_I = 0.2$ .

where

$$d\phi_p = \frac{1}{32\pi^2} \beta(\sqrt{q^2} + m_1, M_I) \beta(\sqrt{q^2} - m_1, M_I) d\Omega_p,$$

$$d\phi_d = \frac{1}{32\pi^2} \beta(m_2 + m_3, \sqrt{q^2}) \beta(m_2 - m_3, \sqrt{q^2}) d\Omega_d.$$

$M_{\text{eff}}^2$  is thus obtained via maximization of

$$\text{PS}(q^2)D(q^2) \propto \frac{\beta(\sqrt{q^2} + m_1, M_I) \beta(\sqrt{q^2} - m_1, M_I) \beta(m_2 + m_3, \sqrt{q^2}) \beta(m_2 - m_3, \sqrt{q^2})}{(q^2 - M^2)^2 + M^2 \Gamma^2}.$$

In Fig. 7, we compare the error of the phase-space improved and standard NWA when the kinematic bounds are approached. It shows that the effective-mass method mitigates the error  $|R|$  to less than  $3\Gamma/M$  for  $M$  arbitrarily close to the kinematic bounds. The divergence of the standard NWA error in this region is also clearly visible. With increasing distance to the kinematic bounds, on the other hand, the PSINWA and standard NWA results converge and are both of  $\mathcal{O}(\Gamma/M)$ .

The PSINWA is general in the sense that the effective mass does not depend on the process matrix elements, and as effective-mass method it preserves the on-shell simplifications of the standard NWA. The former strength is, however, also a potential shortcoming, since for some processes Breit-Wigner deformation is also caused by the  $q^2$ -dependence of the residual matrix elements, which may have to be taken into account to achieve the desired

approximation accuracy. As long as the deformed Breit-Wigner shape is still strongly peaked, the proposed method can be extended: a process-specific effective mass can be calculated by maximizing  $f(q^2) := D(q^2)\text{PS}(q^2)|\mathcal{M}(q^2)|^2$  (and possibly also treating the width as free parameter).<sup>12</sup> For cases where the Breit-Wigner deformation is so severe that a modified mass is not sufficient to obtain the desired accuracy, it may be possible to successfully apply the process-specific method proposed in Ref. [17].

## V. SUMMARY

We studied the general properties of the NWA with polarization/spin decorrelation. After defining the NWA and clarifying the treatment of polarization and spin correlations, we proved for sufficiently inclusive rates of arbitrary resonant decay and scattering processes with an on-shell intermediate state decaying via a cubic or quartic vertex that decorrelation effects vanish and the NWA is of order  $\Gamma$ . When applied in perturbative calculations, the NWA uncertainty is commonly estimated as between  $\approx \Gamma/M/3$  and  $\approx 3\Gamma/M$ . We tested this assumption by systematically determining the NWA accuracy numerically for all resonant 3-body decays involving scalars, spin- $\frac{1}{2}$  fermions or vector bosons. We found that the approximation error will exceed the  $\mathcal{O}(\Gamma/M)$  estimate for mass configurations in an extended vicinity of segment kinematic bounds. This is due to a significant distortion of the Breit-Wigner peak and tail, which is effected by the  $q^2$ -dependence of the phase-space elements and the residual matrix elements. While factorizing coupling parameters do not affect the relative NWA error, for processes with SFF or VFF vertices a strong dependence on the relative strength of the chiral couplings can exist. We specialized the general results to MSSM benchmark scenarios and presented results for SPS 1a. We found that significant off-shell corrections can occur – similar in size to QCD corrections. To simplify a combined treatment we proposed a modified, process-independent approximation that exhibits an improved accuracy close to kinematic boundaries while preserving the simplifying power of the standard NWA.

---

<sup>12</sup> For more complicated phase spaces and/or matrix elements the function to maximize, namely  $f(q^2)$ , may not be available in analytical form. The computation of  $M_{\text{eff}}^2$  will then be more expensive.

## Acknowledgments

We thank the referee for bringing Ref. [8] to our attention. This work was supported by the BMBF, Germany (contract 05HT1WWA2).

- 
- [1] B. C. Allanach *et al.*, arXiv:hep-ph/0402295; B. C. Allanach *et al.*, arXiv:hep-ph/0602198; M. M. Nojiri *et al.*, arXiv:0802.3672 [hep-ph].
  - [2] M. J. G. Veltman, *Physica* **29** (1963) 186.
  - [3] G. Lopez Castro, J. L. Lucio and J. Pestieau, *Mod. Phys. Lett. A* **6** (1991) 3679; U. Baur, J. A. M. Vermaseren and D. Zeppenfeld, *Nucl. Phys. B* **375** (1992) 3; M. Nowakowski and A. Pilaftsis, *Z. Phys. C* **60** (1993) 121 [arXiv:hep-ph/9305321]; A. Denner, S. Dittmaier, M. Roth and D. Wackerath, *Nucl. Phys. B* **560** (1999) 33 [arXiv:hep-ph/9904472].
  - [4] A. P. Chapovsky, V. A. Khoze, A. Signer and W. J. Stirling, *Nucl. Phys. B* **621** (2002) 257 [arXiv:hep-ph/0108190]; M. Beneke, A. P. Chapovsky, A. Signer and G. Zanderighi, *Phys. Rev. Lett.* **93** (2004) 011602 [arXiv:hep-ph/0312331]; M. Beneke, A. P. Chapovsky, A. Signer and G. Zanderighi, *Nucl. Phys. B* **686** (2004) 205 [arXiv:hep-ph/0401002]; A. Denner, S. Dittmaier, M. Roth and L. H. Wieders, *Nucl. Phys. B* **724** (2005) 247 [arXiv:hep-ph/0505042].
  - [5] M. A. Gigg and P. Richardson, arXiv:0805.3037 [hep-ph].
  - [6] H. Pilkuhn, *The interactions of hadrons*, North-Holland, Amsterdam, 1967.
  - [7] D. Berdine, N. Kauer and D. Rainwater, *Phys. Rev. Lett.* **99** (2007) 111601 [arXiv:hep-ph/0703058]; N. Kauer, *Phys. Lett. B* **649** (2007) 413 [arXiv:hep-ph/0703077].
  - [8] D. A. Dicus, E. C. G. Sudarshan and X. Tata, *Phys. Lett. B* **154** (1985) 79.
  - [9] E. Byckling and K. Kajantie, *Particle Kinematics*, John Wiley & Sons Ltd., 1973.
  - [10] G. C. Cho, K. Hagiwara, J. Kanzaki, T. Plehn, D. Rainwater and T. Stelzer, *Phys. Rev. D* **73** (2006) 054002 [arXiv:hep-ph/0601063].
  - [11] M. Muhlleitner, A. Djouadi and Y. Mambrini, *Comput. Phys. Commun.* **168** (2005) 46 [arXiv:hep-ph/0311167].
  - [12] J. Rosiek, *Phys. Rev. D* **41** (1990) 3464; J. Rosiek, arXiv:hep-ph/9511250.
  - [13] C. F. Uhlemann, *Narrow-width approximation in the MSSM*, Diplomarbeit, Fakultät für Physik und Astronomie, Universität Würzburg, 2007

- [<http://theorie.physik.uni-wuerzburg.de/TP2/publications/Dipl/Uhlemann-dipl.pdf>].
- [14] B. C. Allanach *et al.*, in the *Proceedings of APS/DPF/DPB Summer Study on the Future of Particle Physics (Snowmass 2001)*, Snowmass, Colorado, USA, July 2001, p. 125 [arXiv:hep-ph/0202233].
- [15] B. C. Allanach, *Comput. Phys. Commun.* **143** (2002) 305 [arXiv:hep-ph/0104145].
- [16] J. A. Aguilar-Saavedra *et al.*, *Eur. Phys. J. C* **46** (2006) 43 [arXiv:hep-ph/0511344].
- [17] N. Kauer, *JHEP* **0804** (2008) 055 [arXiv:0708.1161 [hep-ph]].